Comparison of Contact Force Evolution Characteristics During Ore Drawing Process Between Short-hole Shrinkage Method and Synchronous Filling Shrinkage Method

[1]Liu Enjiang, [2]Chen Qingfa, [3]Khalid A.M. Salih

[1]Postgraduate, [2]Professor, [3]Postgraduate,

[1] College of Resources, Environment and Materials, Guangxi University, Nanning, China.

Abstract: The flexible isolation layer is laid in advance before a large number of ore drawing in synchronous filling shrinkage method, which overcomes the shortcomings of short-hole shrinkage method in ore drawing process, but also causes significant changes in ore drawing law. With the help of discrete element software PFC, this paper attempts to compare the evolution characteristics of contact force between short-hole shrinkage method and synchronous filling shrinkage method. The results showed that: During the ore drawing process of the two mining methods, the strength variation law of different types of contact force in the bulk medium system is exponential decay, but the distribution law of contact force strength under different node conditions is highly similar. In the process of drawing with short-hole shrinkage method, the direction of contact force network gradually deviates from the vertical direction to the horizontal direction, while in the process of synchronous filling shrinkage method, the direction of contact force network always tends to the horizontal direction. During the drawing process of the two mining methods, the distribution direction of contact force presents obvious stage change, and the variation law of contact force distribution direction and the variation law of anisotropic degree parameter are different in each stage. The research results have great significance to expound the ore flow law in the drawing process of synchronous filling shrinkage method.

Key words: Short-hole shrinkage mining method, synchronous filling shrinkage method, granular materials, contact force, compare

I. INTRODUCTION

In the context of the increasingly safe, efficient, green and harmonious development of mining technology, Professor Chen Qingfa proposed the idea of "simultaneous filling" mining technology in 2010, and at the same time, a representative mining method with synchronous filling shrinkage method as the core is proposed. Because the flexible isolation layer is laid on the surface of ore before a large amount of ore drawing, and when a large amount of ore is drawing, with the help of a vibration drawing machine to make the filling material and the ore sink uniformly and synchronously, which overcomes the shortcomings of short-hole shrinkage method, such as a large number of surrounding rock falling, moving in a large range, ore dilution, funnel blockage and so on. However, it is also affected by the flexible barrier, the flow law of the granular materials (ore) during the ore drawing process of the synchronous filling shrinkage method is obviously different from the flow law of the granular materials during the ore drawing process of the Short-hole shrinkage mining method. The granular materials involved in the ore drawing process of the two mining methods have typical multi-scale (micro-meso-macro) structural framework characteristics, among them, the micro-scale contact force as the basis of the multi-scale structure of the granular materials system is not only a prerequisite for subsequent research, but also has a profound impact on the final macro-scale manifestation of the granular materials system.

In this paper, PFC^{2D} software is used to study the contact force characteristics of granular media system in the process of synchronous filling shrinkage method and short-hole shrinkage method. The parameters of contact force probability distribution density, contact force component ratio and contact force direction distribution in the process of ore drawing are quantitatively calculated, it is hoped that understanding the difference in the micromechanical change law of granular medium system between synchronous filling shrinkage method and short-hole shrinkage method by comparing the evolution characteristics of contact force, and further strengthen the cognition of ore flow law in the drawing process of synchronous filling shrinkage method.

II. CONSTRUCTION OF NUMERICAL TEST MODEL

Based on the recommendations of related literature, selecting the anti-rolling linear contact model to simulate the contact between ore particles to offset the influence of ore particle morphology on the flow of ore particles. The construction process of the numerical test model for ore drawing is carried out in the following three steps:

(1) Wall generation

Use the "wall create" command to construct a numerical test model of single hopper drawing with a length of 168cm, a width of 128cm, and a spacing of 24cm. The side wall of the whole model is composed of 23 walls, of which the bottom is composed of ore exits with the same size, and numbered from 1 to 7 from left to right. There is a total of 21 walls in the mine outlets; the remaining 2 walls represent the side walls of the numerical test model.

(2) Initial particle formation

A number of ore particles are generated in the range of 0.08 cm to 130 cm in the y-axis direction of the wall model by the ball generation command. The gravitational acceleration of these ore particles is $g=9.81 m \cdot s^{-2}$, and their meso-mechanical parameters are shown in Table 1. To efficiently fill and compact the ore particles in the granular media system, the contact model of initial particles is set as a linear contact model, and the friction coefficient between the particles is 0.3. Meanwhile, to conveniently observe the flow phenomena of the ore particles during the drawing process, after the model is balanced, the particles are given different colors at intervals of 10 cm, and the ore particles above 128 cm in the y-axis direction are deleted.

(3) Computation of the particle formation:

After the model is balanced, the particle contact model is changed from the linear contact model to the anti-rolling linear contact model. At this time, the meso-mechanical calculation parameters of the particles in the dispersive medium system are shown in Table 2. When simulating the shallow hole retention method, after opening No. 4 ore port, the ore port is opened, ore particles are released from the ore port, and the ore flow starts immediately. When simulating the synchronous filling and retaining method, use the "Cubic" command to generate a row of 250cm long and 0.0015cm radius above the ore particles, using parallel-bonded fine particles to simulate a flexible isolation layer, and the isolation layer is meso-level, the mechanical parameters are shown in Table 3. At the same time, in order to realize the simulation of the simultaneous filling effect, after each ore drawing, an appropriate amount of filled waste rock particles are generated on the flexible isolation layer (the meso-mechanical parameters and the ore particles in the calculation process are the same), after the model is balanced under its own weight, delete the excess filling particles.

The completed ore drawing numerical test model is shown in **Fig.1**.

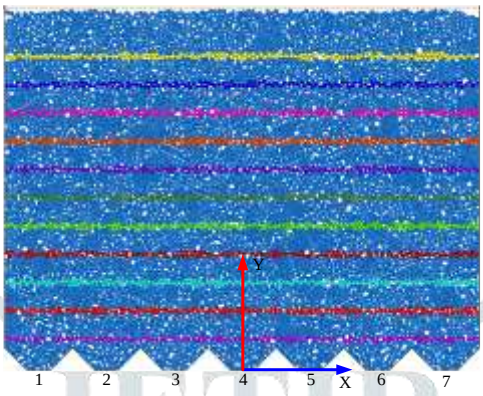

Fig.1 numerical test model of ore drawing

III. RESEARCH ON CONTACT FORCE CHARACTERISTICS

3.1 Evolution of contact force intensity

The contact force between particles plays an important role in the force transmission process in the bulk medium system. The contact force network formed by the contact force between particles is also considered to be an important factor affecting the macroscopic performance of the bulk medium system. However, due to the uneven spatial distribution of the contact network, it is very difficult to directly describe the contact force network. The distribution probability function of the contact force can reflect the distribution of the contact force in the bulk medium system from the angle of the contact force. Based on this, the probability density of contact force distribution is selected to study the strength of contact force between particles.

As a way to simplify calculations, normalization can make data processing more convenient and faster, and the change law obtained after normalization of the data is consistent with the original data law, which can well reflect the changes in the original data law. Therefore, the probability density distribution curve of contact force in this article is the function curve of probability P and M (M is the ratio of the contact force to the mean value of the contact force) obtained by normalizing the contact force in the particle system according to its mean value. Here, we take the total contact force as an example to illustrate the calculation process of normalizing the probability density of contact force.

$$f_i^s = \frac{F_i^s}{\sum F_i^s / N} \qquad (1)$$

Among them, superscript *s* denotes the total contact force, subscript *i* denotes the contact number, f_i^s denotes the normalized normal contact force of contact *i*, F_i^s denotes the normal contact force of contact *i*, and *N* denotes the total number of similar contacts. Similarly, the normal contact force and tangential contact force of normalized contact are f_i^n and f_i^t, respectively.

After normalizing all the total contact forces using Equation 1, the normalized value of all total contact forces can be obtained. Divide the normalized value into several intervals with 0.5 as the interval, the probability density of the total contact force in each interval is obtained by counting the total number of total contact forces after normalization of each interval.

$$P_k^s = \frac{N_k^s}{N^s} \qquad (2)$$

Among them, P_k^s is the probability of the total contact force in the *k* interval, N_k^s is the total contact force in the *k* interval, and N^s is the total contact force in all intervals. Similarly, the probability density of normal contact force and tangential contact force can be obtained as P_k^n and P_k^t, respectively.

According to the above calculation process, the PFC^{2D} software is used to obtain the relevant data of the normal contact force, tangential contact force and total contact force between particles under the conditions of each ore drawing node in the two mining methods. The probability distribution of the contact force intensity is statistically shown in **Fig.2**.

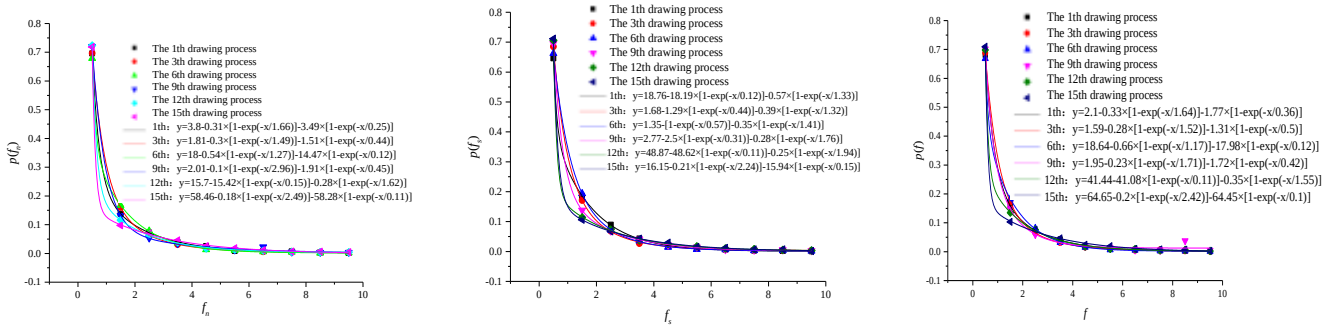

normal contact force tangential contact force total contact forces

(a) probability distribution of contact force in the process of drawing with short-hole shrinkage mining method

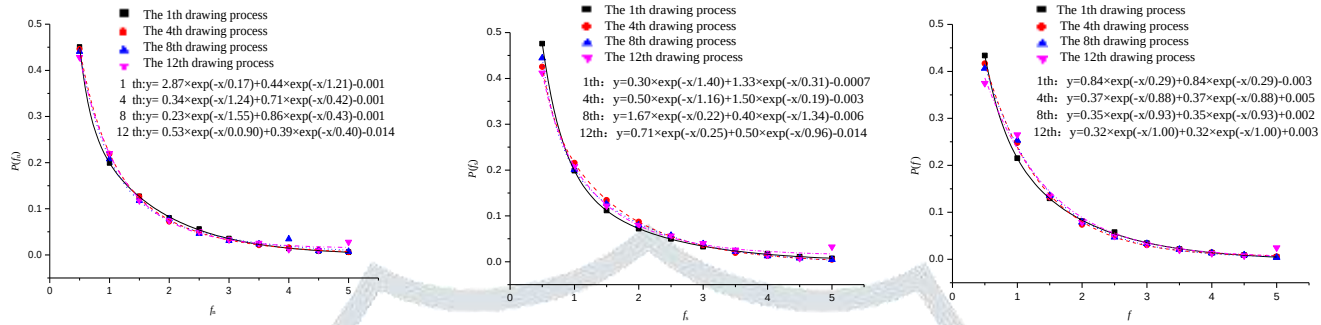

normal contact force tangential contact force total contact forces

（b）probability distribution of contact force during ore drawing process of synchronous filling shrinkage method

Fig.2 probability distribution of contact force

It can be seen from **Fig.2** that after the mean value normalization is used, the changes in the normal direction, tangential direction, and total contact force within the bulk medium system during the synchronous filling shrinkage method, and the short-hole shrinkage mining method are very similar. i.e., the change law of normal contact force, tangential contact force, and total contact force strength all attenuate exponentially. Therefore, the statistical data of the contact force in the ore drawing process are fitted, and the fitting function $y=A_1+A_2\times exp(-x/t_1)+A_3\times exp(-x/t_2)$ is obtained. The fitting coefficients R^2 are all above 0.99, which quite fits the results.

In addition, it can be found from **Fig.2** that whether it is the short-hole shrinkage mining method or the synchronous filling method, the proportion of contact force intensity in the range of 0 to 2 under different node conditions during the ore drawing process is large, while the proportion of contact force intensity in the range of 2 to 5 is small. This phenomenon indicates that in the process of drawing ore with the two mining methods, there are fewer strong power chains in the granular medium system, and most of the power chains are composed of weak power chains. The power chain network formed by the interweaving of strong and weak power chains maintains the entire granular medium system. At the same time, the contact force under the conditions of different ore drawing nodes shows a highly similar change pattern, which also indicates that the process of breaking and reorganization of the force chain continues to occur within the entire granular medium system, and most of the ore particles released during the ore drawing process belong to the particles that form weak force chains.

3.2 Contact network morphology evolution law

The contact force component ratio can quantitatively characterize the overall extension direction of the contact force network shape by the relationship between the contact force components in the x-axis direction and the y-axis direction. The calculation method is as follows:

$$Q_c = \frac{\sum f_i^x - \sum f_i^y}{\sum f_i^x + \sum f_i^y} \qquad (3)$$

where f_i^x denotes the component of the contact force numbered i in the x-axis direction, f_i^y denotes the component of the contact force numbered i in the y-axis direction, and Q_c denotes the component ratio of contact force. When $Q_c > 0$, the contact force deviates in the horizontal direction (i.e., the x-axis direction). When $Q_c < 0$, the contact force deviates in the vertical direction (i.e., the y-axis direction). The greater the difference between Q_c and 0, the greater the degree to which the contact force is deviated in a certain direction.

In order to quantify the evolution characteristics of the contact force network during the drawing process, Equation 3 is used to make statistics on the x-axis and y-axis components of the contact force, as shown in **Fig.3**.

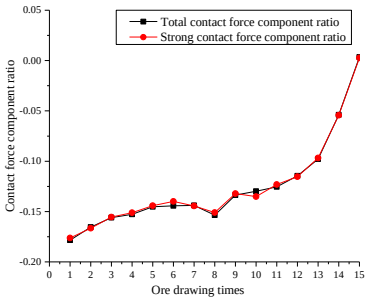

(a)Variation law of contact force component ratio during ore drawing process of short-hole shrinkage method

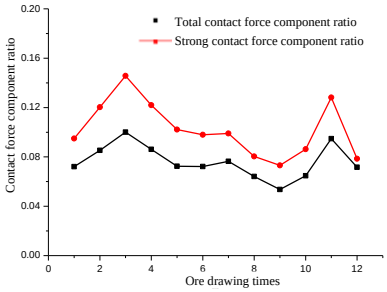

(b)variation law of contact force component ratio during ore drawing process of synchronous filling method

Fig.3 change law of contact force component ratio

It can be seen from **Fig.3(a)** that in the process of drawing with short-hole shrinkage mining method, before the end of 14 times of drawing, the ratio of the total contact force component and the ratio of the strong contact force component are both less than 0. It shows that before the end of 14 times of drawing, the direction of the contact force network within the granular medium system is always biased towards the *y*-axis direction (vertical direction). This is because before the start of ore drawing, the bulk medium system is in the original equilibrium state. Under the influence of the particle's own gravity, the direction of the contact force network inside the system is always biased to the *y*-axis direction. As the ore draw progresses, the ore particles are gradually released, the system's own gravity decreases, and the ratio of the total contact force component to the strong contact component ratio gradually increases due to the influence of factors such as the ore port and the surface morphology of the system. At the end of the 15th draw, there were very few ore particles in the system, and the draw opening became the main factor affecting the direction of the contact force network, making the ratio of the total contact force component and the strong contact component greater than 0, and the direction of the contact force network within the granular medium system is also biased to the *x*-axis direction (horizontal direction).

For the synchronous filling method, it can be seen from **Fig.3(b)** that the component ratios of the total contact force and strong contact force in the granular medium system are all greater than 0, and the component ratio of the strong contact force is approximately 2% larger than that of the total contact force. This shows that the direction of the contact force network in the granular medium system is always biased in the direction of the *x*-axis, and the strong contact force mainly bears the load in the vertical direction. The change rule of the component ratio of the strong contact force and total contact force are consistent. The strong contact force and total contact force fluctuate with increasing ore drawing times, and the fluctuation range is larger in the early and late stages but smaller in the middle stage. This indicates that the contact force network in the granular medium system is constantly changing during the process of ore drawing, that is, the position of the particles is also constantly changing. In the early stage of ore drawing, a granular medium system is released under the action of vertical loads, such as self-gravity and the equivalent load of the ore drawing hole. Then, with the continuous ore drawing, the overlying load and the transverse friction from the isolation layer increase gradually, so the component ratio of the contact force decreases gradually after the rapid rise. In the middle stage of ore drawing, the load in the system gradually stabilizes, so the fluctuation range in the contact force direction is small. In the late stage of ore drawing, influenced by the shape of the isolation layer, the direction of the force acting on the granular medium in the upper part of the isolation layer changes dramatically, so the component ratio of the contact force gradually stabilizes after a slight wave motion.

3.3 The evolution law of the contact network direction

In order to understand the change law of the direction distribution of the contact force network within the granular medium system during the drawing process of the two mining methods, taking 10° as an interval, the 360° is divided into 36 intervals, and the contact number and contact force of ore particles in each interval are counted. Taking the normal contact force as an example, the statistical distribution diagram of the normal contact force between particles under different ore drawing nodes is drawn. At the same time, in order to quantitatively describe the change law of the normal contact force, based on previous research results, the statistical results of normal contact force between particles are fitted using Equation (4). The fitting results are shown in **Fig.4**, Table 4 and Table 5.

$$f_n(\theta) = f_0\left[1 + a_n \cos(\pi \frac{\theta - \theta_n}{\omega})\right] \qquad (4)$$

In the formula, $f_n(\theta)$ is the distribution function of the normal contact force between particles, f_0 is the average value of the normal contact force between all particles in the granular medium system, a_n is the degree of anisotropy coefficient, and the magnitude of a_n represents the degree of anisotropy of the normal contact force, θ_n is the main direction of the force chain distribution in the granular medium system, ω is the periodic control coefficient of the trigonometric function.

It can be seen from **Fig.4(a)** and Table 4 that in the process of drawing with short-hole shrinkage mining method, the normal contact force in the initial stage of drawing shows obvious anisotropy, the average contact force along the *y*-axis is greater than the average along the *x*-axis contact force, the normal contact force between ore particles is mainly concentrated in the vertical direction. As the ore draw progresses, the ore particles in the mine room gradually decrease. Affected by the weight of ore particles, sidewall of the funnel outlet and local residual ore, the normal contact force at an angle of 30° with the horizontal direction gradually increased, and the contact force direction also changed from one to three. In the late stage of drawing, there were very few ore particles in the ore room, and the sidewall of the funnel outlet became the main influence, making the normal contact force with an angle of 45° in the horizontal direction gradually increased, and the contact force direction also changed from three to six. According to the fitting results, it can be seen that from the 1th draw to the end of the 9th draw, the fitting graph of the distribution of the normal contact force between the ore particles is peanut-shaped, and the value of the anisotropy degree a_n increases from 0.22 to 0.42, the main direction of the contact force has also been maintained at about 90°. From the 9th draw to the end of the 12th draw, the normal contact force at an angle of 30° with the horizontal direction gradually increased, and the normal contact force distribution direction also gradually changed from a single plumb direction to a multi plumb direction with an angle of ±30° with the horizontal direction, the

fitting graph of the distribution of the normal contact force between ore particles is petal-shaped, the value of the anisotropy degree a_n becomes 0.38, and the main direction of the normal contact force also changes from 88.14° to 44.28°. From the beginning of the 13th ore drawing to the end of the entire drawing process, the normal contact force at an angle of 45° to the horizontal direction gradually increased, and the distribution direction of the normal contact force gradually changed from three to six. The fitting graph of the distribution of the normal contact force direction is petal-shaped, the anisotropy degree a_n is reduced to 0.25, and the main direction of the normal contact force also changes from 44.28° to 28.24°.

For the synchronous filling method, according to **Fig.4(b)** and Table 5, it can be seen that the normal contact force at the initial stage of drawing shows obvious anisotropy, that is, the average contact force along the *y*-axis is greater than the average contact force along the *x*-axis, and the normal contact force is mainly concentrated in the vertical direction. With the progress of ore drawing, the normal contact force at an angle of 60° with the horizontal direction gradually increased, the main direction of normal contact force distribution changed from one to three, and the degree of anisotropy gradually increased. According to the fitting results, it can be seen that from the beginning of the 1th ore drawing to the end of the 8th ore drawing, the fitting figure shows a peanut-shaped distribution, the anisotropic coefficient increases gradually with the increase in the ore drawing times, and the main direction angle remains at approximately 90°. From the end of the 8th ore drawing to the end of the 12th ore drawing, the fitting figure gradually changes from peanut- shaped to petal- shaped, the anisotropic coefficient continues to increase, and the main direction angle changes from 93.42° to 47.65°; this indicates that the anisotropy of the direction distribution of the contact force in granular medium system increases gradually with the progress of ore drawing, and the contact force intensity in horizontal direction increases gradually. From the above analysis, it can be seen that the normal contact force mainly bears the load in the vertical direction at the initial time. Then, with the continuous release of ore particles, the isolation layer gradually bends and sinks, and the load perpendicular to the isolation layer gradually increases. The normal contact force also begins to distribute along the direction perpendicular to the isolation layer, the contact force intensity at an angle of ±60° in the horizontal direction gradually increases.

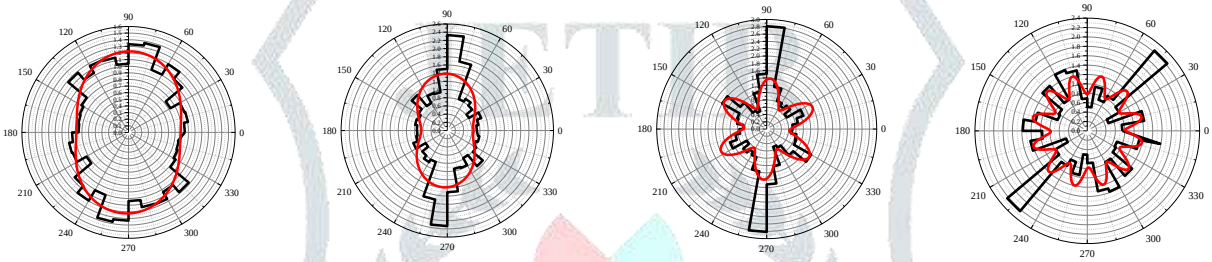

The 1th drawing process The 9th drawing process The 12th drawing process The 15th drawing process

（a）distribution diagram of normal contact force in the process of drawing with short-hole shrinkage mining method

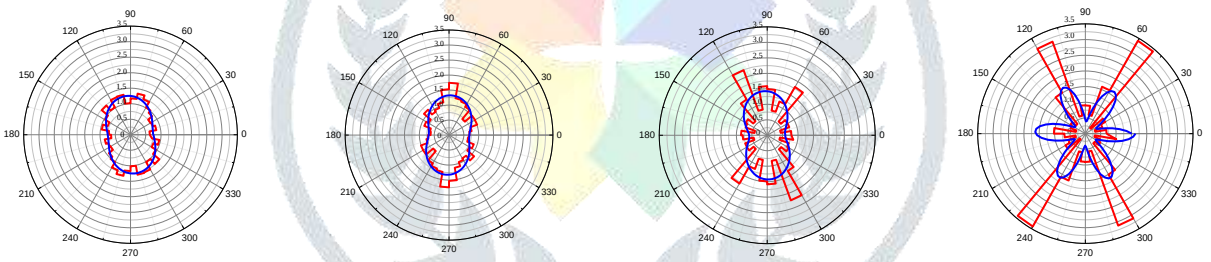

the 1th drawing process The 4th drawing process The 9th drawing process The 12th drawing process

（b）distribution diagram of normal contact force during drawing process with synchronous filling method

Fig.4 distribution of normal contact force under different conditions of drawing nodes

Table 4 Fitting results of normal contact force direction during ore drawing process of short-hole shrinkage method

ore drawing times	f_0	a_n	θ_n	ω
1	1.00	0.22	87.12	90
3	1.00	0.31	86.84	90
6	1.00	0.37	88.58	90
9	1.00	0.42	88.14	90
12	1.00	0.38	44.28	30
15	1.00	0.25	28.24	15

Table 5 Fitting results of normal contact force direction during ore drawing process of synchronous filling method

ore drawing times	f_0	a_n	θ_n	ω
1	1.00	0.26	97.35	90
4	1.00	0.32	85.89	90
8	1.00	0.43	93.42	90
12	1.00	0.61	47.65	30

CONCLUSION

(1) In the process of synchronous filling method and short-hole shrinkage mining method, the change law of normal contact force, tangential contact force, and total contact force in the granular materials system is very similar, in other words, the change law of normal contact force, tangential contact force and total contact force strength all attenuate exponentially; at the same time, the distribution law of contact force strength under different node conditions in the process of drawing is also highly similar.

(2) During the draw process of short-hole shrinkage mining method, at the end of the 14th ore drawing, the ratio of the total contact force component and the strong contact component ratio are both less than 0, and the direction of the contact force network within the granular materials system is always biased towards the *y*-axis direction (vertical direction). With the progress of ore drawing, to the end of the 15th ore drawing, the ratio of the total contact force component and the strong contact component ratio are both greater than 0, and the direction of the contact force network within the granular materials system is also biased to the *x*-axis direction (horizontal direction). But in the process of synchronous filling method, the total contact force component ratio and the strong contact force component ratio in the bulk medium system are both greater than 0, and the direction of the contact force network in the granular materials system is always biased to the *x*-axis direction.

(3) In the process of drawing with short-hole shrinkage mining method, the normal contact force distribution direction gradually evolved from the single-plumb direction at the initial stage of ore drawing to a three-plumb direction, and from three to six at the final stage of drawing, which shows obvious periodic changes. In the process of synchronous filling method, the normal contact force distribution direction only gradually evolves from the single-plumb direction at the initial stage of ore drawing to three-plumb direction, which also presents an obvious periodic change rule. For the anisotropy degree characterization parameter a_n, the two mining methods show different changes in each stage.

REFERENCES

[1] Chen Q F, Wu Zhongxiong. A large number of ore drawing synchronous filling no-top-pillar shrinkage stoping method: CN, 201010181971.2[P]. 2010−10−20.
[2] Chen Q. F, Qin S. K, Chen Q. L. 2019. Numerical simulation of ore particle flow behaviour through a single drawpoint under the influence of a flexible barrier[J]. Geofluids, 2019(1):6127174.
[3] Chen Q. F, Qin S. K, Chen Q. L. 2019. Stress analysis of ore particle flow behaviour under the influence of a flexible barrier[J]. Arabian Journal of Geosciences, 12(15):472.
[4] Chen Q. F, Zhao F. Y, Chen Q. L, et al. 2017. Orthogonal simulation experiment for flowing characteristics of ore-rocks in ore drawing and its influencing factors in single funnel under the flexible isolation layer[J]. JOM, 69(12): 2485-2491.
[5] Wensrich C M, Katterfeld A. 2012. Rolling friction as a technique for modelling particle shape in DEM[J]. Powder Technology, 217: 409-417.
[6] Radjai F, Wolf D E, Jean M, et al. 1998. Bimodal character of stress transmission in granular packings[J]. Physical review letters, 80(1): 61-64.
[7] Majmudar T, Behringer R. 2005. Contact force measurements and stress-induced anisotropy in granular materials[J]. Nature, 435(7045): 1079-1082.
[8] Ostojic S, Somfai E, Nienhuis B. 2006. Scale invariance and universality of force networks in static granular matter[J]. Nature, 439(7078): 828-830.
[9] Emilien Azéma, Radja F. 2012. Force chains and contact network topology in sheared packings of elongated particles[J]. Physical Review E Statal Nonlinear & Soft Matter Physics, 85(3): 31303.
[10] Liu C H, Nagel S R, Schecter D A, et al. 1995. Forcre fluctuations in bead packs[J]. Science, 269(5223): 513-515.
[11] Rothenburg L, Bathurst R J. 1989. Analytical study of induced anisotropy in idealized granular materials[J]. Geotechnique, 40(4): 665-667.